Journal of Theoretical Biology 432 (2017) 38–48

Contents lists available at ScienceDirect

Journal of Theoretical Biology

journal homepage: www.elsevier.com/locate/jtbi

Sink or swim? Vertical movement and nutrient storage in phytoplankton

James P. Grover

Biology Department, University of Texas at Arlington, Box 19498, Arlington, TX 76019 USA

ARTICLE INFO

Article history:
Received 15 March 2017
Revised 21 July 2017
Accepted 12 August 2017
Available online 14 August 2017

Keywords:
Resource competition
Resource storage
Spatial variation
Vertical migration
Water column

ABSTRACT

A simulation model of vertically migrating phytoplankton is presented, using a Lagrangian, individual-based computational approach. Algal cells acquire and store nutrient at the bottom of the habitat, using stored nutrient to grow while in shallower waters. Stored nutrient also governs movement: cells sink when their nutrient quota falls below a threshold; otherwise they rise (or at least sink more slowly). Although the bottom of the habitat provides the growth-limiting nutrient, it also entails a risk of mortality. For a parameter set representing phosphorus-limited algae with a fixed nutrient storage capacity, neither continual sinking nor continual rising are optimal strategies. Instead, an adaptive dynamics approach suggests there is an optimal movement strategy in which cells rise when their storage capacity is partially filled, and otherwise sink. When the movement strategy is fixed in such a way and storage capacity is free to evolve, storage capacity approaches an optimal value several times higher than the minimal quota permitting population growth. Vertical movement and nutrient storage affect the vertical distribution of total nutrient. When cells always sink, total nutrient declines exponentially from the nutrient source at the bottom to a surface minimum. When cells always rise, there is a peak of total nutrient at the bottom, and another at the surface, with a minimum between. When cells move optimally, the vertical distribution of total nutrient can be close to uniform, or have a peak at mid-depth.

© 2017 Elsevier Ltd. All rights reserved.

1. Introduction

Storing resources potentially allows individuals to increase fitness at times and places where the environmental availability of resources is low. Such increased fitness during scarcity comes with costs of synthesizing and maintaining storage products, and allocating resources to storage also entails forgoing the fitness benefits of immediate growth or reproduction. Despite these potential costs, theoretical models of phytoplankton populations competing for nutrients predict that high storage capacity contributes to competitive fitness when nutrient resources become available as large pulses of low or intermediate frequency (Grover, 1991a; Edwards et al., 2012). Conversely, when resource supply is constant, occurs in small frequent pulses, or is very infrequent, strategies of high nutrient affinity or high growth rate with low storage capacity are favored. Several experimental studies of interspecific competition support such differentiations in resource storage and competitive fitness in relation to temporal variation in resource supply (Olsen et al., 1989; Grover, 1991b; Spijkerman and Coesel, 1996; Ducobu et al., 1998).

Planktonic microorganisms experience temporal variations in resource supply in well mixed habitats because of episodic inflows, upwelling, or events of entrainment of deep, nutrient rich water (Soranno et al., 1997; Robarts et al., 1998; Kamarainen et al., 2009). In less well mixed habitats, individuals experience variation in resource supply as they move between regions of higher and lower resource availability. Intuitively, resource storage should be beneficial whether temporal variation in resource supply arises from externally driven variation in a spatially uniform habitat, or from individual movement in a spatially heterogeneous habitat. But this is not necessarily so. In a mathematical model of a water column in which nutrient was supplied only at the bottom and turbulent dispersion moved individuals along random trajectories between nutrient-rich and nutrient-poor locations, storage capacity contributed little to competitive fitness (Grover, 2009). A later study introduced temporal variation in the nutrient source at the bottom of the water column (Grover, 2011), and obtained results similar to those found in well mixed habitats: pulses of high nutrient supply at the right frequency imparted a competitive advantage to resource storage.

These previous studies of partially mixed water columns considered phytoplankton with only two simple types of movement. Sinking carried individuals towards the bottom of the habitat,

E-mail address: grover@uta.edu

http://dx.doi.org/10.1016/j.jtbi.2017.08.012
0022-5193/© 2017 Elsevier Ltd. All rights reserved.

while turbulence interrupted this descent with random displacements of sufficient magnitude to enable populations to persist and spread across all depths. In reality, vertical movements of phytoplankton are more complex. Many cyanobacteria adjust buoyancy to either sink or float (Klemer, 1985; Oliver, 1994; Villareal and Carpenter, 2003). Some eukaryotic algae without flagella can also adjust buoyancy (Villareal et al., 1996), and flagellated eukaryotes can swim up or down (Sommer and Gliwicz, 1986; Hall and Paerl, 2011; DeNoyelles et al., 2016).

The vertical movement behavior of phytoplankton potentially enhances fitness through exploitation of heterogeneous water columns. Near surface locations generally have sufficient light and warm temperature to permit growth while deeper locations are darker, colder, and possibly inviable. In water bodies sufficiently isolated from inflows, nutrient supply comes largely from the bottom due to decomposition and upwelling, and near-surface waters are nutrient depleted. Phytoplankton thus face a dilemma: deep nutrient rich locations put fitness at risk due to other factors, while nutrient-depleted surface waters are otherwise favorable for growth. Classical studies of foraging demonstrate that organisms can balance such spatially conflicting pressures on fitness by adjusting their movements between different parts of the habitat (e.g. Stich and Lampert, 1981; Werner et al., 1983). Thus it is not surprising that phytoplankton have evolved behaviors enabling movement between deep and shallow locations.

This theoretical study examines a corollary hypothesis arising from such behaviors – that storing resources enhances fitness by allowing acquisition in a risky part of the habitat for later use in a more benign location. Phytoplankton populations reside in a partially mixed water column, where a growth-limiting nutrient becomes available only at the bottom (Fig. 1A). Such circumstances are common in productive, seasonally stratified lakes (Wetzel, 2001); a particularly well-studied example is Esthwaite Water (UK) (Sholkovitz and Copland, 1982). Individuals acquiring the nutrient near the bottom have enhanced mortality risk, because transport below the bottom of the habitat removes them altogether. The bottom may be a hydrodynamic barrier (e.g. a thermocline) delineating a depth below which resuspension cannot occur, or the bottom may be too dark and cold for viability, or it may be inhabited by grazers (e.g. bivalves). Mathematically, the bottom is an absorbing boundary for individuals, whose absolute mortality is obviously a convenient caricature of these realistic mortality processes. The parameters describing this habitat are assigned to represent a typical thermally-stratified eutrophic lake (Wetzel, 2001).

As in many previous studies, phytoplankton are modeled as acquiring varying amounts of nutrient per cell, with the amount acquired determining the reproductive rate (Droop, 1968; Grover 1991a, 2009). Depleted individuals sink towards a nutrient source at the bottom. Those that survive the risk of mortality near the bottom and replenish their nutrient quota either rise towards the surface, or at least sink more slowly to make resuspension by turbulence more likely. Such behavior is seen among cyanobacteria that acquire phosphorus and nitrogen in the deeper waters of stratified lakes, using the latter nutrient to build gas vesicles that enable flotation, which then collapse during rapid photosynthesis in surface waters (Klemer, 1985; Villareal and Carpenter, 2003). There are also observations of eukaryotic phytoplankton rising when nutrient-replete and sinking otherwise (Cullen and Horrigan, 1981; Villareal et al., 1996). Such movements might enhance fitness by decoupling nutrient uptake at depth from growth nearer the surface, and can also translocate nutrients towards the surface (Osgood, 1988; Head et al., 1999; Salonen and Rosenberg, 2000). The parameters of algal growth and movement were assigned to represent phosphorus-limited, freshwater algae (Morel, 1987; Edwards et al., 2013), particularly buoyancy-adjusting cyanobacteria.

This study asks two primary questions relating to vertical movement in partially mixed water columns. What is the optimal regulation of such movement, in relation to individual nutrient storage? And what is the optimal resource storage capacity, given such regulated movement behavior? Some attendant questions are also addressed. Given such movement behavior, what is the effect on population and nutrient distribution over the water column? And what is the variation of nutrient quotas among individuals sampled at different locations? The results suggest that there is an optimal strategy for regulating upward and downward motion in relation to stored nutrient quota, and also an optimal storage capacity given a movement behavior. Different vertical movement behaviors and storage strategies, optimal or not, distribute populations and cell-bound nutrients in different vertical patterns. And populations sampled at different locations are predicted to have different nutrient quota distributions among individuals that should be detectable with emerging technologies for interrogating individual cells (Heldal et al., 2003; Bucci et al., 2012; Malerba et al., 2016).

2. Methods

This study extends a Lagrangian model of phytoplankton population growth in a partially mixed water column with a single limiting nutrient (Grover, 2009). The Lagrangian approach represents the heterogeneity of stored resource among individuals taking different trajectories through the habitat and thus encountering different nutrient availabilities. To represent the range of possible trajectories through the habitat, each population (resident or invader) is divided into a large number of homogeneous subpopulations of size $n_i(t)$ (cells), for $i = 1, \ldots, M$ (see Table 1 for notation), with nutrient cell quota $q_i(t)$ (mol cell^{-1}). Each subpopulation moves along the vertical dimension x (m), sinking or rising at a rate $v(q_i)$ (m d^{-1}) according to its respective movement strategy, with random displacements due to turbulent dispersion at a rate δ (m^2 d^{-1}). Using an adaptive dynamics approach and pairwise invasibility plots (Brännström et al., 2013), competitive outcomes are analyzed for a resident population following one movement or storage strategy, invaded by a population following another strategy.

Along its travels, a subpopulation encounters the nutrient at a concentration $R(x,t)$ (mol m^{-3}), which it takes up at a rate

$$\rho(R, q_i) = \left(\frac{R}{K_\rho + R}\right)\left[\rho^{\mathrm{hi}}_{\max} - (\rho^{\mathrm{hi}}_{\max} - \rho^{\mathrm{lo}}_{\max})\left(\frac{q_i - q_{\min}}{q_{\max} - q_{\min}}\right)\right]. \quad (1)$$

This uptake rate (mol cell^{-1} d^{-1}) is a saturating function of R, with half-saturation constant K_ρ (mol m^{-3}), and a linearly decreasing function of q_i, through the term in square brackets (Morel, 1987). This latter term describes a maximal, nutrient saturated uptake rate that varies between two limits, $\rho^{\mathrm{hi}}_{\max}$ and $\rho^{\mathrm{lo}}_{\max}$, as the quota of stored nutrient varies between its limits, $q_{\min}$ and $q_{\max}$. The reproductive rate (d^{-1}) of the population depends on nutrient quota (Droop, 1968):

$$\mu(q_i) = \mu'_{\max}\left(1 - \frac{q_{\min}}{q_i}\right), \quad (2)$$

where the asymptotic growth rate $\mu'_{\max}$ is the reproductive rate (d^{-1}) that would occur with infinite quota. When Eq. (1) is used with Eq. (2), the parameter $\mu'_{\max} = \rho^{\mathrm{lo}}_{\max}/(q_{\max} - q_{\min})$, and is higher than the true maximum rate of reproduction, $\mu_{\max} = \rho^{\mathrm{lo}}_{\max}/q_{\max}$, which occurs at the limit of nutrient storage capacity, $q_i = q_{\max}$ (Morel, 1987). The dynamics of cell numbers and quotas for each subpopulation thus follow

$$\frac{dn_i}{dt} = \mu(q_i) n_i \quad (3a)$$

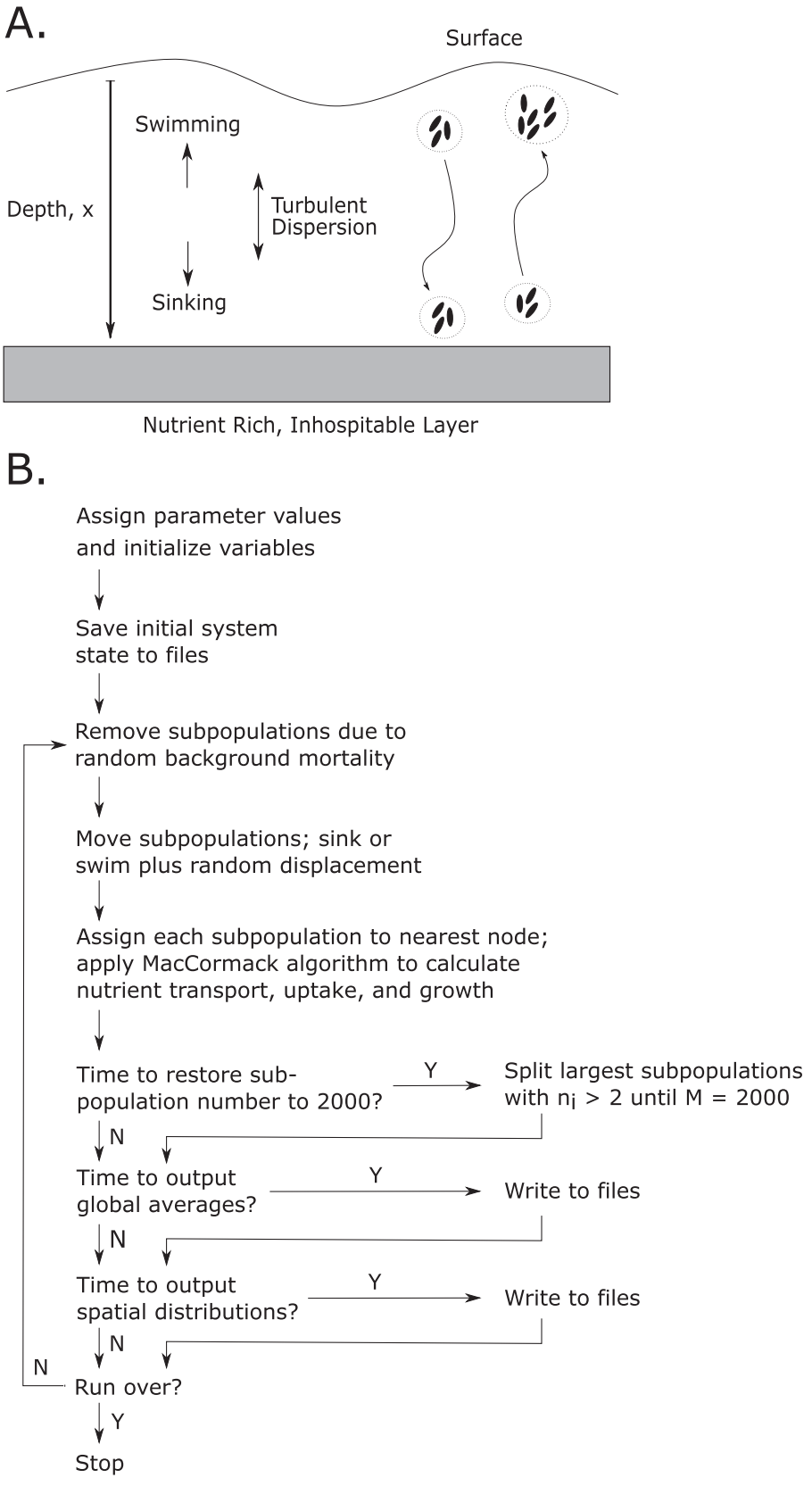

Fig. 1. The biological and computational bases of this study: panel A – Algal populations (shown right side of figure) move through a water column between the surface and bottom boundaries; panel B –flow of computational procedures for a single model run.

Table 1
Notation and default parameter values.

Symbol	Meaning	Default value
Independent variables:		
x	Depth	varies
t	Time	varies
Δx	Grid interval for depth in simulations	0.2 m
Δt	Time interval in simulations	0.001 d
i	Index for subpopulations	ranges 1 to M
Variables:		
$n_i(t)$	Size of subpopulation i	varies
$q_i(t)$	Nutrient quota for cells in subpopulation i	varies
$v(q_i)$	Vertical movement rate for subpopulation i	varies
$R(x,t)$	Nutrient concentration	varies
$\rho(R,q_i)$	Nutrient uptake rate	varies
$\mu(q_i)$	Reproductive rate	varies
ϕ_i	Binary indicator for location of subpopulation i at a given spatial node	0 or 1
Constants:		
M	Number of subpopulations	2000
K_ρ	Half saturation constant for nutrient uptake	0.001 mol m^{-3}
$\rho_{\max}^{\text{lo}}$	Lower bound for nutrient saturated uptake rate	21.6×10^{-15} mol cell^{-1} d^{-1}
$\rho_{\max}^{\text{hi}}$	Upper bound for nutrient saturated uptake rate	660×10^{-15} mol cell^{-1} d^{-1}
$q_{\min}$	Lower bound for nutrient quota	3×10^{-15} mol cell^{-1}
$q_{\max}$	Upper bound for nutrient quota	47.5×10^{-15} mol cell^{-1}
$\mu'_{\max}$	Theoretical maximal population growth rate at infinite quota	0.486 d^{-1}
$\mu_{\max}$	True maximal population growth rate	0.455 d^{-1}
δ	Turbulent dispersion rate	3 m^2 d^{-1}
z	Depth of the water column	10 m
S	Nutrient supply at the bottom of the water column	0.001 mol m^{-3}
v_{sink}	Rate of movement when sinking	0.5 m d^{-1}
v_{swim}	Rate of movement when not sinking	−3 m d^{-1}
q_s	Threshold quota to switch to sinking	15×10^{-15} mol cell^{-1}
m	Background mortality	0.2 d^{-1}

$$\frac{dq_i}{dt} = \rho(R, q_i) - \mu(q_i)q_i. \tag{3b}$$

In the absence of consumption, nutrient concentration follows a simple diffusion equation

$$\frac{\partial R}{\partial t} = \delta \frac{\partial^2 R}{\partial x^2}, \tag{4}$$

with dispersion coefficient δ, a zero-flux boundary condition at the surface ($x = 0$), and a constant source at the bottom ($x = z$) at concentration S (mol m^{-3}):

$$\left.\frac{\partial R}{\partial x}\right|_{x=0} = 0 \tag{5a}$$

$$R(z, t) = S. \tag{5b}$$

In this study, subpopulations are transported randomly with the same diffusivity as nutrients, and either sink at a rate v_{sink} when their quota is at or below a threshold q_s, or otherwise move at a rate v_{swim} ($< v_{\text{sink}}$):

$$v(q_i) = \begin{cases} v_{\text{sink}}, & q_i \le q_s \\ v_{\text{swim}}, & q_i > q_s \end{cases}. \tag{6}$$

The rate v_{swim} may be positive, so that nutrient replete cells sink more slowly than depleted cells, or it may be negative, indicating active movement towards the surface. This movement behavior is assumed to be regulated by internal nutrient status rather than external nutrient availability because there is a large mismatch in spatial scale between an algal cell ($\approx 10^{-5}$ m) and the length over which a vertical nutrient gradient is detectable in aquatic habitats ($\approx$1 m), given turbulent dispersion. Although it is not inconceivable that cells could somehow sense such gradients, information conveyed by intracellular status is more directly accessible: high quota indicates residence in a nutrient rich location, and low quota indicates residence in a sparse location. In habitats where the bottom of the water column is either a dense, nutrient rich water layer or the nutrient rich sediments, a cell sensing that it resides in a sparse location can reliably increase nutrient availability by sinking, at the possible costs of mortality or reduced growth due to low temperature or lack of light. The simple step-function change in movement assumed in Eq. (6) is computationally convenient, and probably best represents flagellated cells that can change their movement very quickly (e.g. Bearon et al., 2004; Sengupta et al., 2017). It is a cruder approximation for organisms that adjust their buoyancy physiologically. For example, construction of gas vesicles in cyanobacteria is not instantaneous (Oliver, 1994).

For numerical studies, the default physiological parameter values for nutrient uptake and growth kinetics used in this study (Table 1) were within the ranges used previously (Grover, 1991a, 2009, 2011) to represent phosphorus-limited phytoplankton (Morel, 1987; Grover, 1989; Edwards et al., 2012, 2013). These default parameters define an alga whose growth rate under constant conditions follows a saturating, Monod function of external nutrient concentration (R) with a true population maximal growth rate of 0.455 d^{-1}, and a half saturation constant of 2.07×10^{-6} mol m^{-3}. Such a species would be a good competitor for phosphorus under spatially uniform, steady state conditions provided its mortality did not approach its maximal growth rate (Grover, 1989). The relative storage capacity of the default alga ($q_{\max}$:$q_{\min} = 15.8$) would also make it a good competitor when nutrient is supplied as large, infrequent pulses (Grover, 1991a; Grover, 2011). Apart from the assignment of a higher value of $q_{\max}$ to the default species, its traits are very close to those of *Anabaena flos-aquae*, a buoyancy-adjusting cyanobacterium.

Physical parameters describing the partially mixed water column habitat were set to values (Table 1) representing typical conditions for thermally stratified inland waters during the growing

season in temperate climate zones, as in previous related studies (Grover, 2009, 2011). The sinking rate (v_{sink}) was set to $0.5\,m\,d^{-1}$, and rate v_{swim} was set to $-3.0\,m\,d^{-1}$. The sinking rate is similar to those used in previous studies (Grover, 2009, 2011), and both rates fall within measured ranges compiled by Reynolds (2006) for freshwater algae, and reflect observations that rates of rising for flagellated algae and buoyant cyanobacteria exceed sinking rates measured for the same organisms. Faster movement speeds up to about $150\,m\,d^{-1}$ occur, for example in marine flagellates (Bearon et al., 2004; Schuech and Menden-Deuer, 2014), and large colonies such as *Trichodesmium* aggregates (Walsby, 1978) and *Rhizosolenia* mats (Villareal et al., 1996).

Computational simulations used minimal modifications of previous procedures (Grover, 2009, 2011) (Fig. 1A). A spatial grid of 51 nodes was used, with 2000 subpopulations for each of two populations with different movement or storage strategies, and a time step Δt of 0.001 d. At the beginning of each time step, movement and mortality were implemented. Each subpopulation was updated to a new position depending on its sinking or rising strategy and turbulent dispersion:

$$x_i(t+\Delta t) = x_i(t) + v\Delta t \pm \sqrt{2\delta\Delta t}, \tag{7}$$

where the sign of the square root was assigned randomly. The boundary at the surface of the water column was reflecting for phytoplankton, so the sign of position x_i was reversed whenever it became negative (above the surface) for any subpopulation. The boundary at the bottom of the water column was absorbing, so any subpopulation reaching a deeper position ($x_i > z$) was removed. In related previous studies (Grover, 2009, 2011), such loss at the bottom was the only mortality process modeled. Populations with a sufficient tendency to rise can escape such mortality and become unbounded, so for this study an additional, spatially uniform process of background mortality was introduced at a per capita rate of $m = 0.2\,d^{-1}$. This rate is within the range of community grazing rates observed for natural communities of herbivorous zooplankton (Sterner, 1989), the most likely cause of such background mortality. In computational simulations, background mortality was enacted by randomly removing subpopulations with probability $m\Delta t$, at the beginning of each time step.

After movement and mortality, each subpopulation was indexed to the nearest spatial node, which is associated with a volume equal to the spatial grid interval Δx, assuming a unit vertical cross-section. Within these volumes, the differential equations for subpopulation and nutrient dynamics were updated using a spatial version of the improved Euler method (MacCormack, 1969; Chapra, 1997). The diffusion equation for nutrients (Eq. (4)) was augmented by the consumption of each subpopulation:

$$\frac{\partial R}{\partial t} = \delta\frac{\partial^2 R}{\partial x^2} - \sum\frac{\phi_i n_i \rho_i}{\Delta x}, \tag{8}$$

where ϕ_i is a binary indicator function that is one for subpopulations associated with a given spatial node and zero otherwise. Thus the sum calculates total consumption by all subpopulations associated with each node.

Every ten time steps, the number of subpopulations was assessed to replace those lost by mortality and restore a minimum of 2000 subpopulations. Replacement was done by sorting subpopulations and splitting the largest until the minimum of 2000 was reached. Daughter subpopulations inherited the same quota and half the population size as parents, and thenceforward followed independent trajectories. To prevent large disparities in subpopulation size, splitting was also implemented if the largest subpopulation exceeded four times the geometric mean for subpopulation size. These rules were modified for populations so small that subpopulations contained few cells. Subpopulations with less than 2 cells were never split, and the number of subpopulations was then allowed to drop below 2000. Simulations of small populations would thus have strong demographic stochasticity, being represented by a small number of subpopulations, each on the order of one individual in size (Grover, 2009). However, the simulations reported here were run with sufficiently large populations that the minimum number of subpopulations was maintained at 2000, avoiding such strong demographic stochasticity.

To assess the fitness of different movement or storage strategies, pairwise invasibility plots (Brännström et al., 2013) were constructed for different strategies of movement regulation, represented by different values of q_s between q_{min} and q_{max} (as assigned in Table 1), and different strategies of nutrient storage, represented by different values of q_{max} between 15 and $85 \times 10^{-15}\,mol\,cell^{-1}$. A resident population following one strategy within the defined range was given 150 to 250 d to reach equilibrium (the longer times were needed when the resident's q_{max} was large). Then, a small population following another strategy was introduced as an invader and its dynamics were simulated for 50 d. As a measure of invader fitness, the slope versus time of the logarithm of the spatially averaged population density was calculated by regression. Usually, the first 20 d of invasion dynamics were discarded because transient changes in subpopulation quotas and numbers were common before a consistent population trend emerged. Output was always graphed and inspected to ensure equilibration of the resident population and estimation of invasion fitness from consistent trends.

Invader populations were introduced with 2000 subpopulations of 5000 cells each, with quotas and positions randomly assigned. These total populations of 10^7 cells were large enough to avoid strong demographic stochasticity even when invader fitness was low. Invader populations had negligible influence on the environment through nutrient consumption compared to residents at equilibrium. Resident populations at equilibrium were typically 10^4 to 10^5 times larger than the invader populations. The Supplementary Material for this article provides source code and an example of the output used in conducting invasion simulations.

Although invader populations were large enough to avoid strong demographic stochasticity, the random walks used to represent turbulent transport of a finite number of subpopulations introduce variation between computational realizations and corresponding estimates of invader fitness. For every combination of resident and invader strategy presented here, invasion fitness estimates from three realizations were averaged. The unavoidable uncertainty in fitness is discussed when presenting results. Given the use of pseudorandom numbers in this study and related ones (Grover, 2009, 2011), it would have been desirable to use the same pseudorandom number generator throughout. Hardware and software upgrades towards the end of this study necessitated replacing an obsolete procedure (drand48, a function not usable with available C compilers for 64-bit Windows systems) with one having similar statistical properties (rand / RAND_MAX procedure, Wilson, 2000). Of the 5760 simulation runs presented in this study, 501 used only the new pseudorandom number generator. For 801 runs performed with both procedures, invader fitness estimates were strongly correlated ($r = 0.988$).

To explore the influence of movement and storage traits on distributions of population and nutrients versus depth, and distributions of quotas among individuals, simulations of monomorphic populations were run to steady state (at least 300 days) for selected trait values.

3. Results

Pairwise invasibility plots were constructed to address two questions: What is the optimal regulation of sinking versus rising? And what is the optimal nutrient storage capacity for cells

that both sink and rise? These questions were analyzed in terms of the traits q_s, the quota below which sinking occurs, and q_{max}, the upper limit on cellular nutrient storage. The first trait, q_s, was allowed to vary between q_{min} and q_{max} (fixing these parameters at the values in Table 1). At one extreme, when $q_s = q_{min}$, cells always rose (at the rate $v_{swim} = -3\,m\,d^{-1}$, Table 1), avoiding mortality at the bottom but risking starvation near the surface. At the other extreme, when $q_s = q_{max}$, cells always sink (at the rate $v_{sink} = 0.5\,m\,d^{-1}$, Table 1), avoiding starvation near the surface but risking mortality at the bottom. For intermediate q_s, cells switched between sinking and rising depending on their quota.

Conventionally, pairwise invasibility plots distinguish invader trait values with positive fitness from those with negative fitness, by coding regions of positive fitness as black and negative fitness as white. Due to stochastic movement and finite computational approximations, invader fitness was determined with uncertainty, as the average from three simulation runs. To present this uncertainty, the pairwise invasibility plot (Fig. 2A) was coded gray where the average of the invader's mean fitness was less than one standard deviation from the three simulations; black and white indicate positive and negative fitness, respectively, greater than one standard deviation in magnitude. The boundaries of these coded regions were jagged due to the randomness of the simulations. Boundaries between positive and negative fitness are uncertain due to this randomness, so data points (simulation runs) underlying the pairwise invasibility plots were heavily clustered around these boundaries.

The gray neutral zone of near-zero invader fitness separated more clearly positive and negative zones. Part of the neutral zone lies along the one-to-one trait line where invader fitness must be zero. Another part of it defined an approximate border whose characteristics indicate potential outcomes of trait evolution. For the trait q_s, this border was a monotonically decreasing curve suggesting a convergence and evolutionarily stable equilibrium (Brännström et al., 2013) at trait value of $q_s \approx 15 \times 10^{-15}\,mol\,cell^{-1}$. The simulation dynamics thus predicted that evolution should approach the neighborhood of this apparent optimum.

With q_s fixed at $15 \times 10^{-15}\,mol\,cell^{-1}$, a second pairwise invasibility plot was constructed for the storage capacity trait q_{max} (Fig 2B). A gray neutral zone again separated black regions of positive invader fitness from white regions of negative fitness, indicating a monotonically decreasing border between positive and negative fitness intersecting a border along the one-to-one line. Thus the evolution of storage capacity should approach the neighborhood of an evolutionarily and convergence stable optimum at $q_{max} \approx 23 \times 10^{-15}\,mol\,cell^{-1}$.

These pairwise invasion plots were constructed by examining mean invader fitness relative to its standard deviation. Alternative visualizations of invader fitness were obtained by fitting a cubic interpolation to mean fitness (not scaled by standard deviation), and then constructing contours from the interpolation (Appendix, Fig. A1). Invaders with strategies near the apparent optima of $q_s \approx 15 \times 10^{-15}\,mol\,cell^{-1}$ and $q_{max} \approx 23 \times 10^{-15}\,mol\,cell^{-1}$ suffered selection weaker than $-0.01\,d^{-1}$. Those with extreme strategies far from optimal suffered selection an order of magnitude stronger.

The movement and nutrient storage strategies adopted by phytoplankton affected their population distribution through the water column, and the vertical distribution of total nutrient concentration (Fig. 3). In all simulations, the dissolved nutrient concentration was predicted to be depleted ($<0.01\,\mu mol\,l^{-1}$) above a depth of about 8 m. Above this depth, the nutrient essentially occurred only in cell-bound form, so that the population distribution was a strong determinant of total nutrient distribution. For a steady state, limiting case where all of the nutrient is cell-bound, background mortality is negligible, and only sinking occurs, total nutrient approximately follows an exponential curve that increases with depth

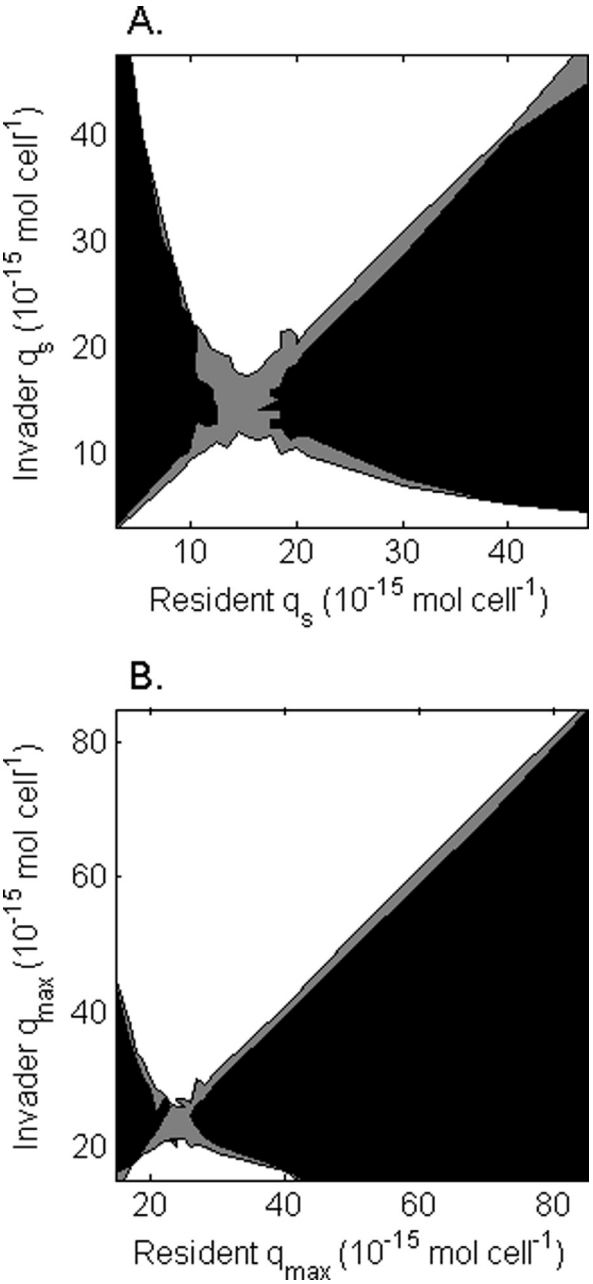

Fig. 2. Pairwise invasibility plots for the traits q_s (panel A) and q_{max} (panel B). Regions coded black indicate the average invader fitness (from three simulation runs) is positive and exceeds one standard deviation in magnitude; regions coded white indicate the average invader fitness is negative and exceeds one standard deviation in magnitude; regions coded gray indicate that average invader fitness is less than one standard deviation in magnitude.

(Appendix A2). A simulation of a population which always sank, with q_s equal to a storage capacity of $q_{max} = 47.5 \times 10^{-15}\,mol\,cell^{-1}$, was distributed with a broad maximum between about 4 and 7 m deep (Fig. 3A, solid line). The corresponding total nutrient concentration followed the predicted exponential relationship with depth (Fig. 3A, dashed line).

In contrast, a population displaying near-optimal regulation of movement with $q_s = 15 \times 10^{-15}\,mol\,cell^{-1}$) and a storage capacity of $q_{max} = 47.5 \times 10^{-15}\,mol\,cell^{-1}$, had a long-term distribution spread more broadly across the upper half of the water column (Fig. 3B, solid line). The corresponding distribution of total nutrient concentration was nearly uniform with depth (Fig. 3B, dashed

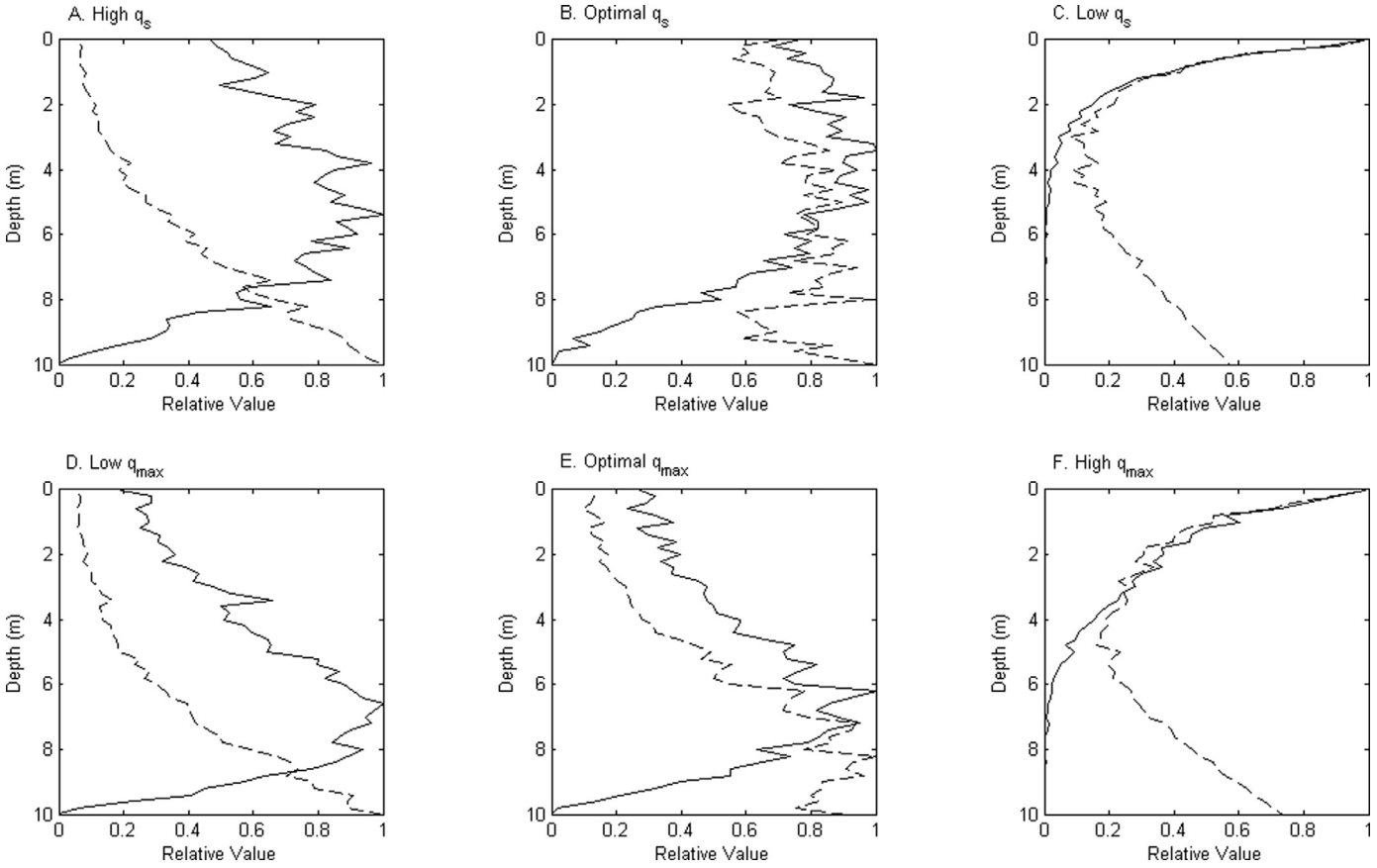

Fig. 3. Vertical distributions of population density (solid lines) and total nutrient concentration (dashed lines) at steady state for various trait values: panel A – $q_s = 85 \times 10^{-15}$ mol cell^{-1}; panel B – $q_s = 15 \times 10^{-15}$ mol cell^{-1}; panel C – $q_s = 3 \times 10^{-15}$ mol cell^{-1}; panel D – $q_{max} = 15 \times 10^{-15}$ mol cell^{-1}; panel E – $q_{max} = 23 \times 10^{-15}$ mol cell^{-1}; panel F – $q_{max} = 85 \times 10^{-15}$ mol cell^{-1}. All other parameters were set to the values in Table 1.

line). Cells that never sank ($q_s = q_{min} = 3 \times 10^{-15}$ mol cell^{-1}) were more closely distributed to the surface (Fig. 3C, solid line), producing a peak of total nutrient concentration near the surface, a minimum of total nutrient about 3–4 m deep, and an increase of total nutrient concentration from there to the bottom (Fig. 3C, dashed line).

For populations regulating movement with $q_s = 15 \times 10^{-15}$ mol cell^{-1}, the value of q_{max} determined how their movements distributed total nutrient over the water column. A storage capacity below-optimal, and equal to q_s ($q_{max} = 15 \times 10^{-15}$ mol cell^{-1}) produced another population that always sank. In this case, its maximum density was relatively deep at about 7 m (Fig. 3D, solid line), and total nutrient concentration again followed an approximately exponential distribution (Fig. 3D, dashed line). With a near-optimal storage capacity of $q_{max} = 23 \times 10^{-15}$ mol cell^{-1}, the population distribution with depth was little changed (Fig. 3E, solid line), but the distribution of total nutrient concentration deviated from exponential, with a peak about 8 m deep (Fig. 3E, dashed line). A similarly-moving population with a very large storage capacity ($q_{max} = 85 \times 10^{-15}$ mol cell^{-1}) above optimal reached its peak at the surface (Fig. 3F, solid line), and produced another example of a total nutrient distribution with a peak at the surface and another at the bottom (Fig. 3F, dashed line). Movement and storage traits also influenced the distributions of cellular nutrient quotas among individuals and across depths (Fig. 4). For all cases examined, the average quota increased with depth, as expected from proximity to the nutrient source, and the dispersion among individuals varied with depth in ways that depended on traits.

4. Discussion

The analysis presented here predicts that in a partially mixed water column whose bottom provides nutrients at the risk of mortality, phytoplankton should neither swim to the surface nor sink to the bottom. Instead, they should regulate their vertical movement so as to maximize fitness by balancing mortality risk against growth opportunities, while using nutrient storage to maintain growth when moving away from risky but rich locations. The regulated movement of phytoplankton is analogous to many observations of other aquatic organisms. Fish adjust their use of resource-rich foraging sites in relation to the risk of predation mortality (Werner et al., 1983; Gilliam and Fraser, 1987; Swain et al., 2015), and herbivorous zooplankton use diel vertical movements to avoid surface waters, rich in algal food, during the daytime when visual predators (fish) can best attack them (Stich and Lampert, 1981; Gliwicz, 1986; Lampert, 1987). It is reasonable to expect that such organisms would also exhibit some degree of nutrient storage.

A number of sophisticated spatial models of phytoplankton dynamics on the vertical dimension have been constructed. However, many of these models either do not address conditional movement behaviors (Cianelli et al., 2009; Grover 2009, 2011), use growth formulations without nutrient storage (Liccardo et al., 2013), or use an approach to storage that averages all individuals' quotas at a given location (Kerimoglu et al., 2012; Frassl et al., 2014). A smaller number of models resolve both resource storage and movement behavior at the individual level using approaches similar to that taken here (Broekhuizen, 1999; Beckman and Hense, 2004; Ross and Sharples, 2008). But to date this approach has not been

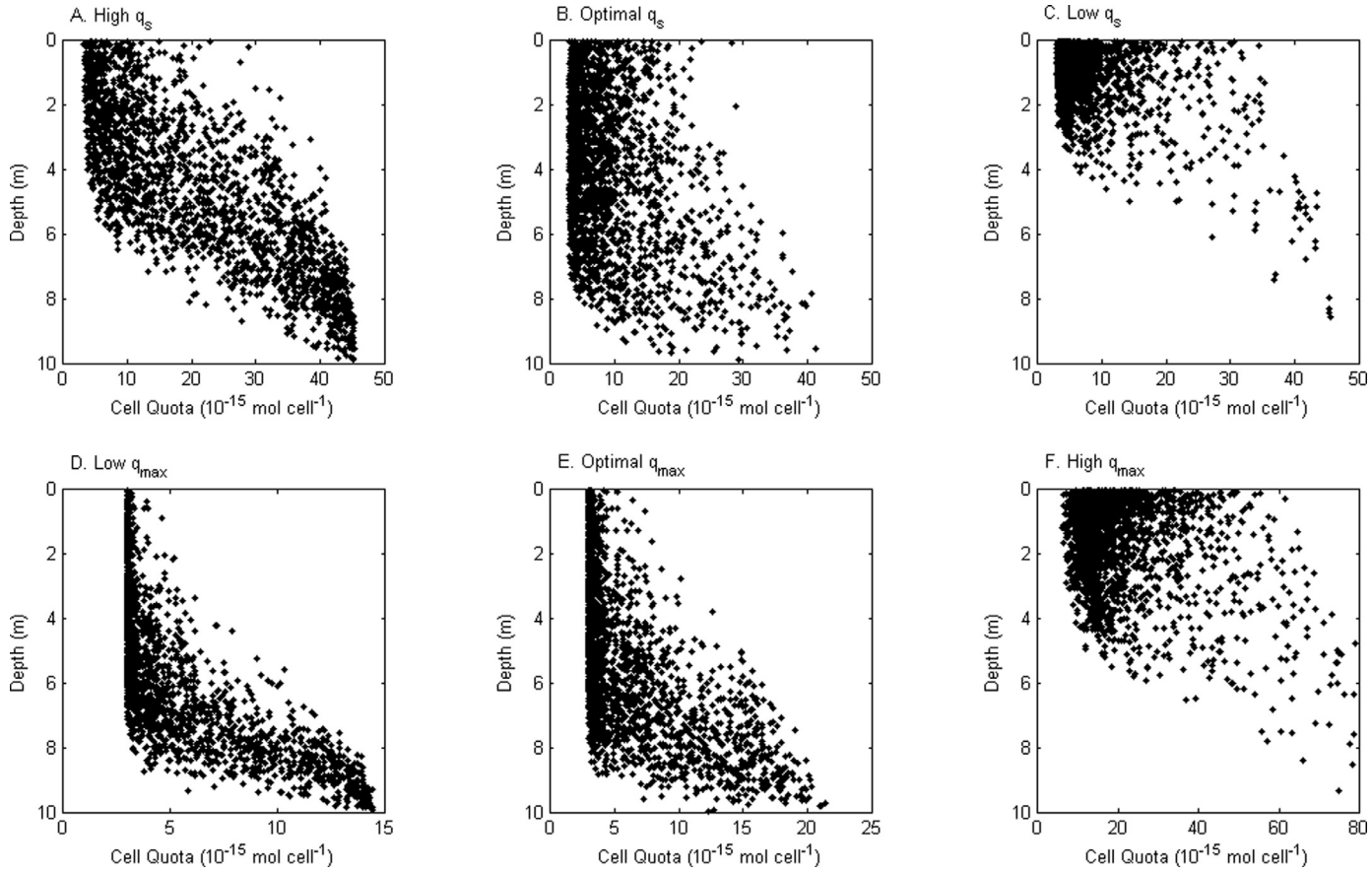

Fig. 4. Distributions of quotas over depth and over subpopulations at steady state for various trait values: panel A – $q_s = 85 \times 10^{-15}$ mol cell^{-1}; panel B – $q_s = 15 \times 10^{-15}$ mol cell^{-1}; panel C – $q_s = 3 \times 10^{-15}$ mol cell^{-1}; panel D – $q_{max} = 15 \times 10^{-15}$ mol cell^{-1}; panel E – $q_{max} = 23 \times 10^{-15}$ mol cell^{-1}; panel F – $q_{max} = 85 \times 10^{-15}$ mol cell^{-1}. All other parameters were set to the values in Table 1.

used to explore the adaptive evolution of movement and storage strategies. More general spatial theory with simple advective and diffusive movements suggests that fitness-maximizing, evolutionarily stable strategies emerge when organisms move in response to fitness-related cues (Cosner and Winkler, 2014; Lam and Lou, 2014). This study has added a detailed consideration of resource storage in this context of balancing growth opportunities and mortality risks across space. Here, resource storage coupled to growth is both a cue for movement, and an evolving trait that can itself affect fitness. This study suggests that resource storage capacity, like movement strategy, approaches an evolutionarily stable optimum.

For the model and parameters adopted here, the apparent optima for the quota at which cells switch to sinking (q_s) and for storage capacity (q_{max}) suggest that movement towards the rich but risky bottom of the habitat should begin at relatively modest reductions in growth. When storage capacity is fixed (at 47.5×10^{-15} mol cell^{-1}), the quota for switching to sinking approaches an optimum at about 15×10^{-15} mol cell^{-1}. This optimum is 27% of full storage capacity, and given the other parameters adopted, produces a 14% reduction below the maximal per capita growth rate. When the quota for switching to sinking is fixed at 15×10^{-15} mol cell^{-1}, resource storage approaches an optimum at about 23×10^{-15} mol cell^{-1}. For this optimal storage capacity, the switch to sinking then occurs at 60% of full storage, and is associated with an 8% reduction below the maximal per capita growth rate. Simulations predict large variations of quota and growth among individuals, with many having growth reduced more than 50% below maximal (Fig. 4). The large differences in nutrient quota and growth rate predicted for individuals at different depths would perhaps be detectable with techniques of single-cell analysis (Heldal et al., 2003; Bucci et al., 2012; Malerba et al., 2016).

The potential generality of the patterns predicted here can be assessed through the dimensionless Péclet number ($\mathrm{Pe} = vz \,/\, \delta$), which is 1.7 for sinking cells and 10 for rising cells. The values of movement speed (v), water column depth (z), and turbulent dispersion (δ) used here represent relatively slow-moving algae in relatively shallow quiescent lakes. However, the associated Pe values fall within the range used in other studies of phytoplankton movement (e.g. Broekhuizen, 1999; Jäger et al., 2010; Liccardo et al., 2013). It is reasonable to expect similar results for parameters characterizing larger lakes and marine systems, especially where faster-moving algae are involved.

The finding that optimal storage capacity (q_{max}) can exceed the quota for switching to sinking suggests that resource storage evolves as an adaptation to permit growth in resource-poor, but low mortality regions of the habitat. For the case examined here, the quota for switching to sinking is 15×10^{-15} mol cell^{-1} and resource storage approaches an optimum at about 23×10^{-15} mol cell^{-1}, so that $q_{max}{:}q_{min} = 7.67$. Interestingly, the optimal storage capacity found here is close to the observed value for the buoyancy-adjusting cyanobacterium *Anabaena flos-aquae* (21×10^{-15} mol cell^{-1}, Morel, 1987), so that the final parameter set closely matches the properties of this species. Storage capacity selected by movement behavior modeled here thus exceeds the minimal nutrient requirement by about 8×, which may be compared to storage capacity selected by other factors. In particular, similar modeling approaches examining habitats supplied

with infrequent nutrient pulses suggests that fitness is highest when storage capacity is 10–12× higher than the minimal nutrient requirement (Grover, 1991a, 2011). Thus it appears that temporal variation in nutrient supply might exert stronger selection for storage capacity than movement to exploit rich but risky regions of the habitat. But none of these theories yet explains the full extent of storage capacity observed in phytoplankton, whose ratios of q_{max}:q_{min} for phosphorus range up to 427 (Grover, 1997).

In this study, variation in storage capacity was explored by changing the parameter q_{max} without any changes in the corresponding parameter governing nutrient uptake capacity (ρ^{lo}_{max}). In the context of the growth model used (Morel, 1987), increased storage capacity thus had high fitness costs of reduced maximal growth rate (μ_{max}) and reduced ability to compete in uniform environments at steady state (i.e. higher R^*, Grover, 1991a). If uptake capacity increased proportionally to storage capacity, such costs would be eliminated and perhaps directional rather than stabilizing selection would occur to increase storage capacity. Even without strict proportionality, some amount of increased uptake capacity correlated with higher storage capacity would decrease the costs of storage and could help to explain the full extent of observed storage capacities. The optimal storage capacity also likely depends on several environmental parameters, and related earlier work suggests that it is higher for intermediate turbulence and deeper mixed depth (Grover, 2011).

In such deeper waters, the vertical separation of light from nutrient sources could potentially explain additional benefits to nutrient storage, beyond those predicted from analyzing nutrients alone. A number of theoretical studies examine light- and nutrient-limited phytoplankton dynamics in spatially explicit, vertically resolved models. However, none of these studies analyzes the contribution to fitness of both vertical movement behavior and nutrient storage as coupled traits. Several studies suggest that vertical migration between nutrient-rich depths and the well-lit surface can enhance fitness, but do not analyze nutrient storage (Broekhuizen, 1999; Beckmann and Hense, 2004; Ross and Sharples, 2008; Yoshiyama et al., 2009). Others suggest that storage can enhance fitness when resources are vertically segregated, but do not analyze vertical movements (Kerimoglu et al., 2012; Frassl et al., 2014). Still other studies address population and competitive dynamics, but do not analyze either nutrient storage or vertical migration (Cianelli et al., 2009; Jäger et al., 2010; Ryabov and Blasius, 2014). A unified exploration of vertical resource segregation, vertical migration, and nutrient storage would appear to be both feasible and enlightening.

Nearly neutral dynamics often emerged for competing populations in this study, as they have in other studies of resource competition across space (e.g. Cianelli et al., 2009; Grover, 2011), but there was no strong prediction of stable coexistence of competitors differentiated by storage or movement strategies. Using movement and storage to exploit spatially varying mortality and resource availability, as constructed here, thus appears to be equalizing rather than stabilizing (sensu Chesson, 2000). In a habitat where a resident superior competitor has established a low average resource availability, an invading inferior competitor can benefit from regions with above average availability, reducing its fitness disadvantage relative to the resident. The concave-down relationship between population growth and acquired nutrient (Eq. (2)) limits such benefits, and hence the scope for stabilization of coexistence. The tendency towards equalization can be important to coexistence, however, because it reduces the strength of stabilization required from other factors not considered here, such as selective predation (Chesson, 2000). Equalization also potentially contributes to maintaining genetic variance in storage and movement traits among phytoplankton.

This study assumes that a resident population reaches an ecological equilibrium before mutation or invasion introduces a second population following a different strategy, and that the invader's strategy is close to that of the resident, as might be produced by mutations of small effect. If the latter assumption of small differences in traits is relaxed, it is possible that an evolutionary singular state is stable against invasion by nearby strategies, but susceptible to invasion by populations pursuing sufficiently different strategies, as might be produced by mutations of large effect (Kremer and Klausmeier, 2013). The pairwise invasion plots presented here (Fig. 2) do not display the geometry characteristic of such local but not global evolutionarily stable states, and global convergence stability is a reasonable interpretation of the results obtained. In the seasonal habitats occupied by many phytoplankton, rapid trait evolution compared to ecological dynamics offers a potential for cycles among evolutionary states permitting coexistence of different strategies (Kremer and Klausmeier, 2013), a possibility not addressed here.

In the simulation protocol used here, relatively large invader populations were used (10^7 total cells, distributed among 2000 subpopulations). In contrast, mutations arise in a single individual. Although the computational method applied here can potentially mimic this phenomenon by running in a mode where subpopulations have approximately one individual (Grover, 2009), the strongly stochastic dynamics of this mode were avoided. Undoubtedly the procedure used overestimates the rate at which competitively superior phenotypes would evolve, though it may more accurately represent the dynamics of new phenotypes arriving through ecological invasions. The stochastic barrier faced by new mutants (or rare invaders) can delay evolutionary branching (Wakano and Iwasa, 2013), but in this study, no potential for such diversification was revealed. The Lagrangian simulation method used here could be used to approximate the probability of mutant survival, by computing its emergent mortality rate and generation time distribution (Powell, 1958), an analysis beyond the scope of this study, which focused on the more deterministic ecological selection taking place after initial survival.

This study examined traits related to movement and nutrient storage one at a time, to maintain analytical focus and computational tractability. It suggests that phytoplankton will evolve regulated movement behaviors and associated nutrient storage strategies that balance mortality risks and growth benefits. But this study did not find pathways to evolutionary branching and diversification for these traits. It is likely that the traits examined here evolve simultaneously. In general, evolution of multiple traits offers more potential for diversification than evolution of a single trait (Doebeli and Ispalatov, 2010; Svardal et al., 2014). Traits of movement and nutrient storage likely evolve in concert with those of light harvesting and carbon fixation, not considered here. Computational improvements will be needed to extend this study's approach to consider multiple resources and traits while resolving nearly neutral dynamics. Using the current program code, the pairwise invasibility plots presented here each took many months to construct (see Supplementary Material). There is a long tradition of mechanistic modeling of ecologically important traits in phytoplankton, which provides a basis for continued study of their evolution, and could yield insights into long-standing questions around the paradoxical diversification of the phytoplankton in seemingly featureless habitats (Hutchinson, 1961; Li and Chesson, 2016).

Acknowledgment

The University of Texas at Arlington supported this research.

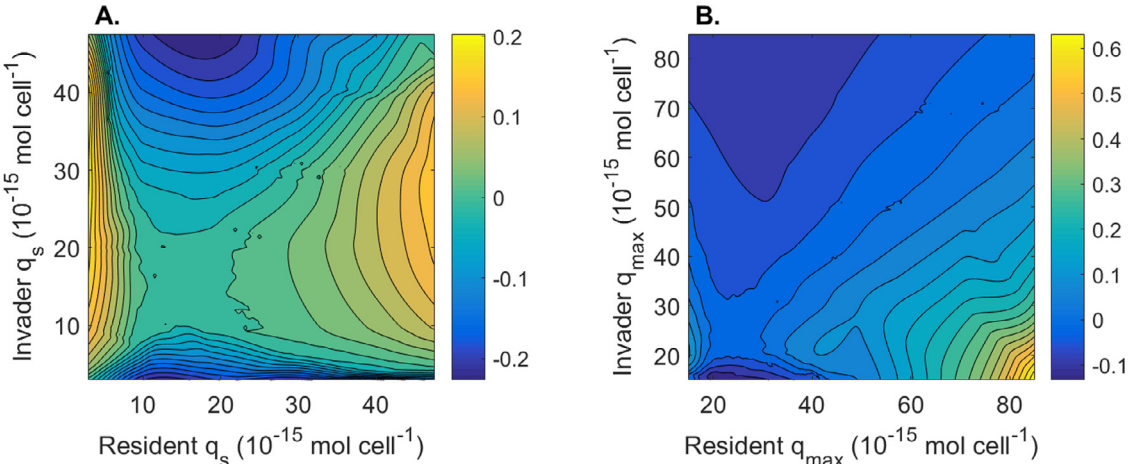

Fig. A1. Contours of invader fitness corresponding to the pairwise invasion plots presented in the main text (Fig. 2).

Appendix

A1. Fitness contours for pairwise invasion plots

Contours of invader fitness (Fig. A1) were estimated from the simulations used to construct pairwise invasion plots (Fig. 2). For each combination of invader and resident traits, invader fitness was estimated as the average of three simulation runs. Three-dimensional fitness surfaces as functions of resident and invader traits were then interpolated using the Matlab function griddata with the cubic option. Twenty-level contour plots of the resulting surfaces were then constructed with the Matlab function contourf. Matlab version R2016a was used.

A2. Analysis of the depth-distribution of total nutrient concentration

Consider a limiting case where the dissolved nutrient concentration is depleted, $R(x,t) \approx 0$ for $0 \le x < z$, cells always sink at a constant rate $v > 0$, and background mortality is negligible ($m \approx 0$). Then, the total nutrient concentration is approximated by $T(x,t) \approx \bar{q}\, N(x,t)$ where $\bar{q}$ is an appropriate average quota. At steady state, the approximate depth distribution of T is thus proportional to that of population density, and so follows the boundary value problem

$$\delta \frac{d^2T}{dx^2} - v\frac{dT}{dx} = 0, \qquad vT(0) - \delta \left.\frac{dT}{dx}\right|_{x=0} = 0, \qquad T(z) = S, \quad \text{(A.1)}$$

which has the solution

$$T(x) = Se^{\frac{v}{\delta}(x-z)}. \quad \text{(A.2)}$$

The approximate steady state distribution for total nutrient thus decreases exponentially from the source concentration (S) at the bottom of the water column ($x = z$), upwards to the surface ($x = 0$), where the total nutrient concentration is $Se^{-vz/\delta}$. In simulations with cells that always sink, this approximation holds well for the long term distribution of total nutrient versus depth (Fig. 3A and D, dashed lines), despite the presence of background mortality and non-negligible dissolved nutrient concentration near the bottom of the habitat.

Supplementary materials

Supplementary material associated with this article can be found, in the online version, at doi:10.1016/j.jtbi.2017.08.012.

References

Bearon, R.N., Grünbaum, D., Cattolico, R.A., 2004. Relating cell-level swimming behaviors to vertical population distributions in *Heterosigma akashiwo* (Raphidophyceae), a harmful alga. Limnol. Oceanograph. 49, 607–613.

Beckman, A., Hense, I., 2004. Torn between extremes: the ups and downs of phytoplankton. Ocean Dynam. 54, 581–592.

Brännström, A., Johansson, J., von Festenburg, N., 2013. The hitchhiker's guide to adaptive dynamics. Games 4, 304–328.

Broekhuizen, N., 1999. Simulating motile algae using a mixed Eulerian-Lagrangian approach: does motility promote dinoflagellate persistence or co-existence with diatoms? J. Plankton Res. 21, 1191–1216.

Bucci, V., Nunez-Milland, D., Twining, B.S., Hellweger, F.L., 2012. Microscale patchiness leads to large and important intraspecific internal heterogeneity in phytoplankton. Aquatic Ecol. 46, 101–118.

Chapra, S.C., 1997. Surface Water-quality Modeling. McGraw Hill, New York.

Chesson, P., 2000. Mechanisms of maintenance of species diversity. Annu. Rev. Ecol. Systemat. 31, 343–366.

Cianelli, D., Sabia, L., d'Alcalà, M.R., Zambianchi, E., 2009. An individual-based analysis of the dynamics of two coexisting phytoplankton species in the mixed layer. Ecol. Modell. 220, 2380–2392.

Cosner, C., Winkler, M., 2014. Well-posedness and qualitative properties of a dynamical model for the ideal free distribution. J. Math. Biol. 69, 1343–1382.

Cullen, J.J., Horrigan, S.G., 1981. Effects of nitrate on the diurnal vertical migration, carbon to nitrogen ratio, and the photosynthetic capacity of the dinoflagellate – *Gymnodinium splendens*. Marine Biol. 62, 81–89.

DeNoyelles, F., Smith, V.H., Kastens, J.H., Bennett, L.A., Lomas, J.M., Knapp, C.W., Bergin, S.P., Dewey, S.L., Chapin, B.R.K., Graham, D.W., 2016. A 21-year record of vertically migrating subepilimnetic populations of *Cyptomonas* spp. Inland Waters 6, 173–184.

Doebeli, M., Ispalotov, I., 2010. Complexity and diversity. Science 328, 494–497.

Droop, M.R., 1968. Vitamin B_{12} and marine ecology. IV. The kinetics of uptake, growth and inhibition in *Monochrysis lutheri*. J. Marine Biol. Assoc. UK 48, 689–733.

Ducobu, H., Huisman, J., Jonker, R.R., Mur, L.R., 1998. Competition between a prochlorophyte and a cyanobacterium under various phosphorus regimes: comparison with the Droop model. J. Phycol. 34, 467–476.

Edwards, K.F., Klausmeier, C.A., Litchman, E., 2013. A three-way tradeoff maintains functional diversity under variable resource supply. Am. Naturalist 182, 786–800.

Edwards, K.F., Thomas, M.K., Klausmeier, C.A., Litchman, E., 2012. Allometric scaling and taxonomic variation in nutrient utilization traits and maximum growth rates of phytoplankton. Limnol. Oceanograph. 57, 554–566.

Frassl, M.A., Rothhaupt, K.-O., Rinke, K., 2014. Algal internal nutrient stores feedback on vertical phosphorus distribution in large lakes. J. Great Lakes Res. 40, 162–172.

Gilliam, J.F., Fraser, D.F., 1987. Habitat selection under predation hazard: test of a model with foraging minnows. Ecology 68, 1856–1862.

Gliwicz, M.Z., 1986. Predation and the evolution of vertical migration in zooplankton. Nature 320, 746–748.

Grover, J.P., 1989. Phosphorus-dependent growth kinetics of 11 species of freshwater algae. Limnol. Oceanograph. 34, 339–346.

Grover, J.P., 1991a. Resource competition in a variable environment: phytoplankton growing according to the variable-internal-stores model. Am. Naturalist 138, 811–835.

Grover, J.P., 1991b. Dynamics of competition among microalgae in variable environments: experimental tests of alternative models. Oikos 62, 231–243.

Grover, J.P., 1997. Resource Competition. Chapman and Hall, London.

Grover, J.P., 2009. Is storage an adaptation to spatial variation in resource availability? Am. Naturalist 173, E44–E61.
Grover, J.P., 2011. Resource storage and competition with spatial and temporal variation in resource availability. Am. Naturalist 178, E124–E148.
Hall, N.S., Paerl, H.W., 2011. Vertical migration patterns of phytoflagellates in relation to light and nutrient availability in a shallow microtidal estuary. Marine Ecol. Progress Series 425, 1–19.
Head, R.M., Jones, R.I., Bailey-Watts, A.E., 1999. Vertical movements by planktonic cyanobacteria and the translocation of phosphorus: implications for lake restoration. Aquatic Conserv. 9, 111–120.
Heldal, M., Scanlan, D.J., Norland, S., Thingstad, F., Mann, N.H., 2003. Elemental composition of single cells of various strains of marine *Prochlorococcus* and *Synechococcus* using X-ray microanalysis. Limnol. Oceanograph. 48, 1732–1743.
Hutchinson, G.E., 1961. The paradox of the plankton. Am. Naturalist 95, 137–145.
Jäger, C.G., Diehl, S., Emans, M., 2010. Physical determinants of phytoplankton production, algal stoichiometry, and vertical nutrient fluxes. Am. Naturalist 175, E91–E104.
Kamarainen, A.M., Penczykowski, R.M., Van de Bogert, M.C., Hansson, P.C., Carpenter, S.R., 2009. Phosphorus sources and demand during summer in a eutrophic lake. Aquatic Sci. 71, 214–227.
Kerimoglu, O., Straile, D., Peeters, F., 2012. Role of phytoplankton cell size on the competition for nutrients and light in incompletely mixed systems. J. Theor. Biol. 300, 330–343.
Klemer, A.R., 1985. Nutrient-induced migrations of blue-green algae (cyanobacteria). In: Rankin, M.A., Checkley, D., Cullen, J., Kitting, C., Thomas, P. (Eds.), Migration: Mechanisms and Adaptive Significance. Contributions in Marine Science 27. University of Texas Marine Science Institute, Port Aransas, Texas, pp. 154–165.
Kremer, C.T., Klausmeier, C.A., 2013. Coexistence in a variable environment: eco-evolutionary perspectives. J. Theor. Biol. 339, 14–25.
Lam, K.-Y., Lou, Y., 2014. Evolution of conditional dispersal: evolutionarily stable strategies in spatial models. J. Math. Biol. 68, 851–877.
Lampert, W., 1987. Vertical migration of freshwater zooplankton: indirect effects of vertebrate predators on algal communities. In: Kerfoot, W.C., Sih, A. (Eds.), Predation: Direct and Indirect Impacts On Aquatic Communities. University Press of New England, Hanover, NH, pp. 291–299.
Li, L., Chesson, P., 2016. The effect of dynamical rates on species coexistence in a variable environment: the paradox of the plankton revisited. Am. Naturalist 188, E1–E13.
Liccardo, A., Fierro, A., Iudicone, D., Bouruet-Aubertot, P., 2013. Response of the deep chlorophyll maximum to fluctuations in vertical mixing intensity. Progress Oceanograph. 100, 33–46.
MacKormack, R.W., 1969. The effect of viscosity in hypervelocity impact cratering. American Institute of Aeronautics and Astronautics Paper 69-354. Reprinted in Journal of Spacecraft and Rockets 40, 757–763 (2003).
Malerba, M.E., Connolly, S.R., Heimann, K., 2016. Standard flow cytometry as a rapid and non-destructive proxy for nitrogen cell quota. J. Appl. Phycol. 28, 1085–1095.
Morel, F.M.M., 1987. Kinetics of nutrient uptake and growth in phytoplankton. J. Phycol. 23, 137–150.
Oliver, R.L., 1994. Floating and sinking in gas-vacuolate cyanobacteria. J. Phycol. 30, 161–173.
Olsen, Y., Vadstein, O., Andersen, T., Jensen, A., 1989. Competition between *Staurastrum leutkemuellerii* (Chlorophyceae) and *Microcystis aeruginosa* (Cyanophyceae) under varying modes of phosphate supply. J. Phycol. 25, 486–499.
Osgood, R.A., 1988. A hypothesis on the role of *Aphanizomenon* in translocating phosphorus. Hydrobiologia 169, 69–76.
Powell, E.O., 1958. Criteria for the growth of contaminants and mutants in continuous culture. J. General Microbiol. 18, 259–268.
Reynolds, C.S., 2006. The Ecology of Phytoplankton. Cambridge University Press, Cambridge.
Robarts, R.D., Waiser, M.J., Hadas, O., Zohary, T., MacIntyre, S., 1998. Relaxation of phosphorus limitation due to typhoon-induced mixing in two morphologically distinct basins of Lake Biwa, Japan. Limnol. Oceanograph. 43, 1023–1036.
Ross, O.N., Sharples, J., 2008. Swimming for survival: a role of phytoplankton motility in a stratified turbulent environment. J. Marine Syst. 70, 248–262.
Ryabov, A.B., Blasius, B., 2014. Depth of the biomass maximum affects the rules of resource competition in a water column. Am. Naturalist 184, E132–E146.
Salonen, K., Rosenberg, M., 2000. Advantages from diel vertical migration can explain the dominance of *Gonyostomum semen* (Raphidiophyceae) in a small, steeply-stratified humic lake. J. Plankton Res. 22, 1841–1853.
Schuech, R., Menden-Deuer, S., 2014. Going ballistic in the plankton: anisotropic swimming behavior of marine protists. Limnol. Oceanograph.: Fluids Environ. 4, 1–16.
Sengupta, A., Carrara, F., Stocker, R., 2017. Phytoplankton can actively diversify their migration strategy in response to turbulent cues. Nature 543, 555–561.
Sholkovitz, E.R., Copland, D., 1982. The chemistry of suspended matter in Esthwaite Water, a biologically productive lake with seasonally anoxic hypolimnion. Geochimica et Cosmochimica Acta 46, 393–410.
Sommer, U., Gliwicz, Z.M., 1986. Long range vertical migration of Volvox in tropical Lake Cahora Bassa (Mozambique). Limnol. Oceanograph. 31, 650–653.
Soranno, P.A., Carpenter, S.R., Lathrop, R.C., 1997. Internal phosphorus loading in Lake Mendota: response to external loads and weather. Canad. J. Fisheries Aquatic Sci. 54, 1883–1893.
Spijkerman, E., Coesel, P.F.M., 1996. Competition for phosphorus among planktonic desmid species in continuous culture. J. Phycol. 32, 939–948.
Sterner, R.W., 1989. The role of grazers in phytoplankton succession. In: Sommer, U. (Ed.), Plankton Ecology: Succession in Plankton Communities. Springer-Verlag, Berlin, pp. 107–170.
Stich, H.-B., Lampert, W., 1981. Predator evasion as an explanation of diurnal vertical migration by zooplankton. Nature 293, 396–398.
Svardal, H., Rueffler, C., Doebeli, M., 2014. Organismal complexity and the potential for evolutionary diversification. Evolution 68, 3248–3259.
Swain, D.P., Benoit, H.P., Hammill, M.O., 2015. Spatial distribution of fishes in a Northwest Atlantic ecosystem in relation to risk of predation by a marine mammal. J. Animal Ecol. 84, 1286–1298.
Villareal, T.A., Carpenter, E.J., 2003. Buoyancy regulation and the potential for vertical migration in the oceanic cyanobacterium *Trichodesmium*. Microbial Ecol. 45, 1–10.
Villareal, T.A., Woods, S., Moore, J.K., Culver-Rymsza, K., 1996. Vertical migration of *Rhizosolenia* mats and their significance to NO_3^- fluxes in the central North Pacific gyre. J. Plankton Res. 18, 1103–1121.
Wakano, J.Y., Iwasa, Y., 2013. Evolutionary branching in a finite population: deterministic branching vs. stochastic branching. Genetics 193, 229–241.
Walsby, A.E., 1978. The properties and buoyancy-providing role of gas vacuoles in *Trichodesmium* Ehrenberg. Brit. Phycol. J. 13, 103–116.
Werner, E.E., Gilliam, J.F., Hall, D.J., Mittelbach, G.G., 1983. An experimental test of the effect of predation risk on habitat use in fish. Ecology 64, 1540–1548.
Wetzel, R.G., 2001. Limnology: Lake and River Ecosystems, third ed Academic Press, San Diego.
Wilson, W., 2000. Simulating Ecological and Evolutionary Systems in C. Cambridge University Press, Cambridge.
Yoshiyama, K., Mellard, J.P., Litchman, E., Klausmeier, C.A., 2009. Phytoplankton competition for nutrients and light in a stratified water column. Am. Naturalist 174, 190–203.